

iconductor particles in aqueous solution.<sup>88</sup> Finally, it should be pointed out that the poor reversibility observed upon electrochemical oxidation may be a major practical limitation, unless appropriate fast oxidation relay species are coupled with these sensitizers.

- (88) Borgarello, E.; Pelizzetti, E.; Ballardini, R.; Scandola, F. *Nouv. J. Chim.* **1984**, *8*, 567.
- (89) The periodic group notation in parentheses is in accord with recent actions by IUPAC and ACS nomenclature committees. A and B notation is eliminated because of wide confusion. Groups IA and IIA become groups 1 and 2. The d-transition elements comprise groups 3 through 12, and the p-block elements comprise groups 13 through 18. (Note that the former Roman number designation is preserved in the last digit of the new numbering: e.g., III → 3 and 13.)

**Acknowledgment.** We thank Dr. M. Ciano for performing the cyclic voltammetry experiments. This work was supported by the Commission of the European Communities (Contract ESD-026-I) and by the Consiglio Nazionale delle Ricerche (Progetto Finalizzato Chimica Fine e Secondaria, Tematica Ah1).

**Registry No.** Al(QO)<sub>3</sub>, 2085-33-8; Rh(QO)<sub>3</sub>, 21689-22-5; Ir(QO)<sub>3</sub>, 15671-12-2; Pt(QO)<sub>2</sub>, 21710-20-3; Pb(QO)<sub>2</sub>, 14976-96-6; Bi(QO)<sub>3</sub>, 16029-28-0; tetracyanoethylene, 670-54-2; 1,4-benzoquinone, 106-51-4; 9,10-phenanthraquinone, 84-11-7; 1,2-dinitrobenzene, 528-29-0; 4-nitrobenzaldehyde, 555-16-8; 4-nitrobenzotrile, 619-72-7; 1,3-dinitrobenzene, 99-65-0; 3-nitrobenzotrile, 619-24-9; 3-nitrobenzaldehyde, 99-61-6; 4-bromo-1-nitrobenzene, 586-78-7; 4-chloro-1-nitrobenzene, 100-00-5; 4-fluoro-1-nitrobenzene, 350-46-9; nitrobenzene, 98-95-3; 4-methyl-1-nitrobenzene, 99-99-0; methylviologen dication, 4685-14-7.

Contribution from the Departments of Chemistry, University of Denver, Denver, Colorado 80208, and University of Colorado at Denver, Denver, Colorado 80202, and Central Laboratory of Chemistry, University of Pecs, 7643 Pecs, Hungary

## Metal-Nitroxyl Interactions. 48. EPR Spectra of Spin-Labeled Pyridines Coordinated to Chromium(III) Tetraphenylporphyrin Chloride ( $S = 3/2$ ) and Comparison of the Electron-Electron Exchange Interaction with Analogous Complexes with Metal $S = 1/2$

Kundalika M. More, Gareth R. Eaton,\* Sandra S. Eaton, and Kalman Hideg

Received March 11, 1986

EPR spectra were obtained for 13 spin-labeled pyridines coordinated to chromium(III) tetraphenylporphyrin chloride. In fluid solution weak electron-electron exchange interaction caused broadening of the nitroxyl signal and stronger interaction caused resolved splitting. Resolved spin-spin splitting was observed in frozen solution. Values of the exchange coupling constant,  $J$ , between  $\pm 0.005$  and  $\pm 0.27$  cm<sup>-1</sup> were obtained by computer simulation of the frozen-solution spectra. The stronger exchange interaction for 4-substituted pyridines than for analogous 3-substituted pyridines is consistent with  $\pi$  delocalization of the unpaired spin density from the metal into the pyridine ring.  $\pi$  delocalization was also dominant in the vanadyl trifluoroacetylacetonate complexes of these spin-labeled pyridines. The values of  $J$  for the Cr(III) ( $S = 3/2$ ) complexes were  $1/2$  to  $2/3$  of the values observed for the vanadyl ( $S = 1/2$ ) complexes of the same spin-labeled pyridines.

### Introduction

Recent studies of homonuclear and heteronuclear metal-metal dimers have shown that the electron-electron exchange interaction decreased as the number of unpaired electrons on the metal increased.<sup>1-5</sup> If the geometry of a metal-nitroxyl complex is held constant and the electron-electron spin-spin interaction involves a single half-filled orbital on the metal, the value of the exchange coupling constant,  $J$ , is expected to be proportional to  $1/n$  where  $n$  is the number of unpaired electrons on the metal.<sup>6</sup> The value of  $n$  cannot be varied experimentally without altering other properties of the metal that may also contribute to changes in the value of  $J$ . When spin-labeled pyridines were coordinated to Mn(II), the value of  $J$  was  $1/4$  to  $<1/50$  of that observed for analogous complexes of Cu(II) and  $1/8$  to  $<1/40$  of that observed for vanadyl.<sup>7</sup> Mn(II) has half-filled d orbitals with both  $\sigma$  ( $d_{z^2}$ ) and  $\pi$  ( $d_{xz}, d_{yz}$ ) symmetry relative to the pyridine orbitals of the spin-labeled ligand. The metal-nitroxyl interaction probably has significant contributions from orbitals of both symmetries. If the resultant contributions to  $J$  were of similar magnitude and of opposite sign, this could cause the value of  $J$  for  $S = 5/2$  Mn(II) to be less than  $1/5$  of the values observed for  $S = 1/2$  Cu(II) or vanadyl. In this context it was of interest to determine how much change in  $J$  would be observed as a function of  $n$  for metal-radical interactions in which the spin-spin interaction was through a single half-filled orbital.

The equilibrium constant for coordination of pyridine to chromium tetraphenylporphyrin chloride (Cr(TPP)Cl) in toluene solution at room temperature is  $2 \times 10^5$ .<sup>8,9</sup> This equilibrium is

sufficiently favorable to permit EPR studies of spin-labeled pyridines bound to Cr(TPP)Cl without interference from large amounts of dissociated nitroxyl or metalloporphyrin. We have therefore examined the EPR spectra of spin-labeled pyridines I-XIII coordinated to Cr(TPP)Cl. We have previously reported the EPR spectra of I-XII bound to copper(II) and vanadyl  $\beta$ -diketonates.<sup>10-14</sup>

### Experimental Section

**Physical Measurements.** EPR spectra were obtained on a Varian E9 interfaced to an IBM CS9000<sup>15</sup> or on an IBM ER200 interfaced to an IBM CS9000. Spectra were obtained with 100-kHz modulation at modulation amplitudes that did not distort the line shapes and microwave

- (1) Lambert, S. L.; Hendrickson, D. N. *Inorg. Chem.* **1979**, *18*, 2683.
- (2) Spiro, C. L.; Lambert, S. L.; Smith, T. J.; Duesler, E. N.; Gagne, R. P.; Hendrickson, D. N. *Inorg. Chem.* **1981**, *20*, 1229.
- (3) Torihara, N.; Okawa, H.; Kida, S. *Chem. Lett.* **1978**, 185.
- (4) O'Connor, C. J.; Freberg, D. P.; Sinn, E. *Inorg. Chem.* **1979**, *18*, 1077.
- (5) Lambert, S. L.; Spiro, C. L.; Gagne, R. R.; Hendrickson, D. H. *Inorg. Chem.* **1979**, *18*, 1077.
- (6) Hay, P. J.; Thibeault, J. C.; Hoffmann, R. *J. Am. Chem. Soc.* **1975**, *97*, 4884.
- (7) More, J. K.; More, K. M.; Eaton, G. R.; Eaton, S. S. *J. Am. Chem. Soc.* **1984**, *106*, 5395.
- (8) Summerville, D. A.; Jones, R. D.; Hoffman, B. M.; Basolo, F. *J. Am. Chem. Soc.* **1977**, *99*, 8195.
- (9) Ozawa, T.; Hanaki, A. *Inorg. Chim. Acta* **1985**, *102*, 169.
- (10) Boymel, P. M.; Eaton, G. R.; Eaton, S. S. *Inorg. Chem.* **1980**, *19*, 727.
- (11) Boymel, P. M.; Braden, G. A.; Eaton, G. R.; Eaton, S. S. *Inorg. Chem.* **1980**, *19*, 735.
- (12) Sawant, B. M.; Shroyer, A. L. W.; Eaton, G. R.; Eaton, S. S. *Inorg. Chem.* **1982**, *21*, 1093.
- (13) More, J. K.; More, K. M.; Eaton, G. R.; Eaton, S. S. *Inorg. Chem.* **1982**, *21*, 2455.
- (14) More, K. M.; Eaton, G. R.; Eaton, S. S. *J. Magn. Reson.* **1984**, *59*, 497.
- (15) Quine, R. W.; Eaton, G. R.; Eaton, S. S. *J. Magn. Reson.* **1986**, *66*, 164.

\* To whom correspondence should be addressed at the University of Denver.

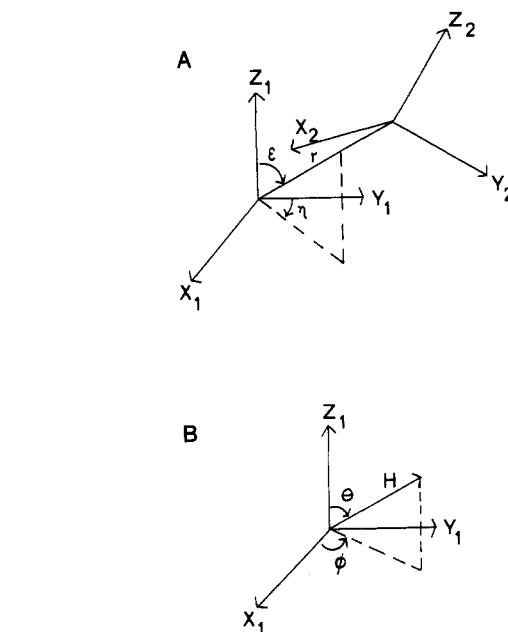
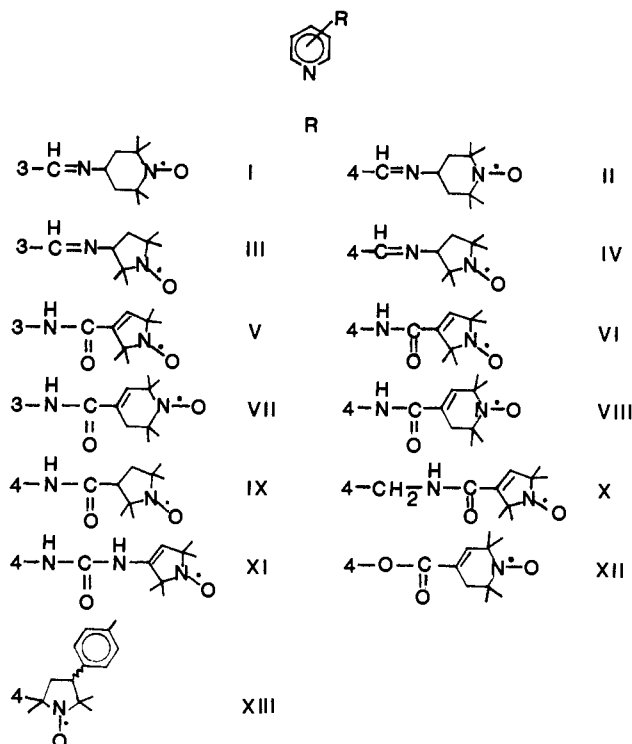


**Figure 1.** Definitions of angles that define the orientation of the interspin vector (A) and magnetic field (B) relative to the axes defined by the chromium zero-field splitting.

powers that did not cause saturation. The solutions used to obtain the spectra contained approximately equimolar Cr(TPP)Cl and spin-labeled pyridine at  $(1-2) \times 10^{-3}$  M in toluene or 2:1 toluene/chloroform. The lines in the spectra were sufficiently broad that degassing the solutions did not change the spectra. Therefore, spectra were obtained on air-saturated solutions.

**Preparation of Compounds.** Compounds were prepared by literature methods cited as follows: Cr(TPP)Cl,<sup>8</sup> I-II,<sup>10</sup> III-IV,<sup>11</sup> V-IX,<sup>12</sup> X-XI,<sup>13</sup> XII.<sup>12</sup>

Compound XIII was prepared by starting with the corresponding  $\alpha,\beta$ -unsaturated ketone, which was converted to the  $\gamma$ -nitro ketone and then to the nitron. Reaction with methylmagnesium iodide resulted in the formation of two isomers: stereoisomer I with mp 106–107 °C; stereoisomer II with mp 68–70 °C. The assignment of the diastereomers and the detailed procedures for preparation of pyridyl-substituted pyrrolidine-1-oxyl derivatives will be published elsewhere.<sup>16</sup>

**Computer Simulations.** The frozen-solution EPR spectra were simulated with a computer program, METNO. The Hamiltonian included the Zeeman interactions for both metal and nitroxyl, the zero-field splitting for the metal, and dipolar and isotropic exchange interaction between the unpaired electrons on the metal and the nitroxyl. Since only <sup>53</sup>Cr (9.5% abundance) has a nuclear spin, nuclear hyperfine interaction with the metal nucleus was not included in the calculations. Hyperfine coupling to the nuclear spin of the nitroxyl nitrogen also was not included. Thus the calculations are only applicable to spectra in which the line widths of the nitroxyl lines and the spin-spin interaction are greater than the nitroxyl nitrogen hyperfine interaction. Since the nitroxyl  $g$  values are nearly isotropic, the orientation of the nitroxyl axes with respect to the axes of the metal were not defined in these calculations. The energy matrix was solved by using Belford's frequency shift perturbation method.<sup>17,18</sup> This procedure uses diagonalization at one magnetic field (for each orientation of the molecule in the magnetic field) and a perturbation calculation of the field-dependent portion of the energy matrix to determine transition energies and transition probabilities. A negative value of  $J$  indicates an antiferromagnetic interaction. The angles used to define the orientation of the interspin vector and the magnetic field relative to the zero-field-splitting axes of Cr(III) are shown in Figure 1.

The following parameters were used for all of the calculated spectra: chromium,  $g = 1.996$ ,  $D = 0.16$  cm<sup>-1</sup>,  $E = 0.013$  cm<sup>-1</sup> (lit.<sup>8</sup> for Cr-

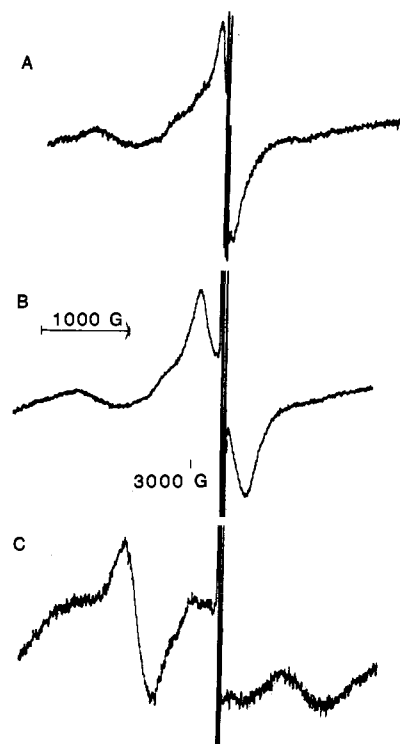


**Figure 2.** X-Band (9.101 GHz) EPR spectra (4000-G scans) of Cr(TPP)Cl-L in fluid solution at room temperature: (A) L = IX, spectrum obtained with 4-G modulation amplitude and 40-mW microwave power; (B) L = VIII, spectrum obtained with 4-G modulation amplitude and 50-mW microwave power; (C) L = IV, spectrum obtained with 4-G modulation amplitude and 20-mW microwave power.

(TPP)Cl.py  $g = 1.995$ ,  $D = 0.158$  cm<sup>-1</sup>,  $E = 0.002$  cm<sup>-1</sup>); nitroxyl,  $g = 2.0059$ . The splitting of the low-field chromium lines in the complexes with the spin-labeled pyridines indicated a larger value of  $E$  than was observed for Cr(TPP)Cl.py. Due to the relatively long interspin distances for most of the complexes, the calculated EPR spectra were not strongly dependent on the values of  $\epsilon$  and  $\eta$ . Although the calculated spectra were sensitive to the relative signs of  $J$  and  $D$ , the differences were not large enough to permit an unambiguous determination of the relative signs. The impact of the choice of magnetic field for diagonalization on the calculated spectra was checked for each complex. Calculated spectra

(16) Hideg, K.; Hankovsky, H. O.; Halasz, H. A., to be submitted for publication.

(17) Belford, R. L.; Davis, P. H.; Belford, G. G.; Lenhardt, T. M. *Extended Interactions Between Metal Ions in Transition Metal Complexes*; ACS Symposium Series 5; American Chemical Society: Washington, DC, 1974; p 40.

(18) Scullane, M. I.; White, L. K.; Chasteen, N. D. *J. Magn. Reson.* **1982**, *47*, 383.

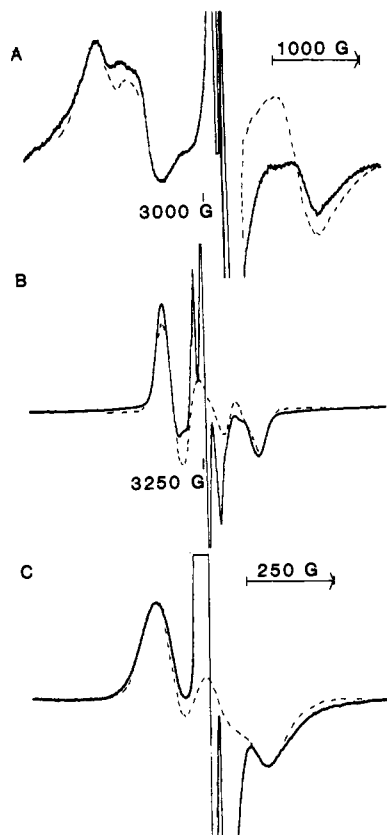


**Figure 3.** X-Band (9.101 GHz) EPR spectra of Cr(TPP)Cl-L in frozen solution at  $-180\text{ }^{\circ}\text{C}$ : (A) 4000-G scan for L = II, obtained with 4-G modulation amplitude and 10-mW microwave power; (B) 4000-G scan for L = II obtained with 2-G modulation amplitude and 1-mW microwave power; (C) 1000-G scan for L = XII, obtained with 4-G modulation amplitude and 5-mW microwave power. The dotted lines indicate regions in which the calculated spectra do not overlay the experimental curves.

were obtained for 90–130 values of  $\theta$  and 20–30 values of  $\phi$ . The calculations required 15–30 min on a VAX 780 or 7–15 min on a Harris H1000.

### Results and Discussion

In an equimolar mixture of Cr(TPP)Cl and spin-labeled pyridine in toluene or 2:1 toluene/chloroform solution at room temperature a few percent of the nitroxyl gave a sharp three-line signal, which indicated that a small amount of the spin-labeled pyridine was not coordinated to Cr(TPP)Cl. The remainder of the nitroxyl signal was broadened and/or shifted due to interaction with the paramagnetic ( $S = 3/2$ ) Cr(III). Three spectra that demonstrate the effects of increasing electron–electron spin–spin interaction on the nitroxyl EPR spectra are shown in Figure 2. Weak interaction causes a broadening of the nitroxyl EPR signal (Figure 2A). As the strength of the interaction increases, the nitroxyl signal splits into two peaks (Figure 2B) and the intensity moves away from  $g = 2$  (Figure 2C). The line widths of the nitroxyl signals in the EPR spectra of Cr(TPP)Cl-L (L = I–XIII) are given in Table I. In fluid solution the EPR signals from Cr(III) are broad and the effects of the spin–spin interaction on the lines are difficult to see.

**EPR Spectra in Frozen Solution.** The frozen-solution EPR spectrum of Cr(TPP)Cl-II is shown in Figure 3A,B. The chromium lines (Figure 3A) are similar to those that were observed for Cr(TPP)Cl-py. A small amount of II that was not coordinated gave a characteristic sharp three-line nitroxyl signal (Figure 3B). Superimposed on that signal was a broader spectrum due to the nitroxyl in the complex. The broad nitroxyl signal was simulated with  $J = 0.0073\text{ cm}^{-1}$ ,  $r = 12\text{ \AA}$ ,  $\epsilon = 25^{\circ}$ , and  $\eta = 75^{\circ}$ . The binding constant was smaller for ligand XII than for ligand II so the signal from nitroxyl that was not interacting with chromium was larger in the spectrum of Cr(TPP)Cl-XII (Figure 3C) than in the spectrum of Cr(TPP)Cl-II (Figure 3B). Although the

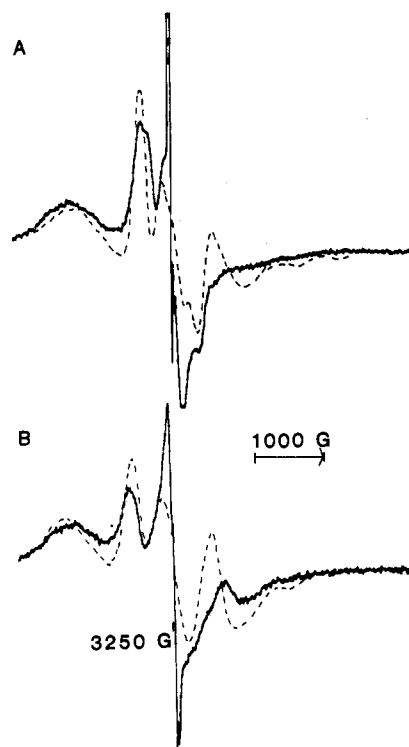


**Figure 4.** X-Band (9.101 GHz) EPR spectra (6000 G scans) of Cr(TPP)Cl-L in frozen solution at  $-180\text{ }^{\circ}\text{C}$ : (A) L = VIII, spectrum obtained with 4-G modulation amplitude and 10-mW microwave power; (B) L = XI, spectrum obtained with 4-G modulation amplitude and 15-mW microwave power. The dotted lines indicate regions in which the calculated spectra do not overlay the experimental curves.

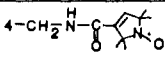
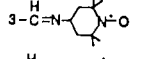
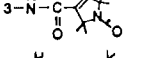
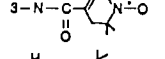
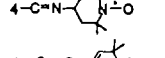
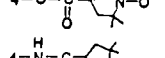
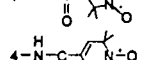
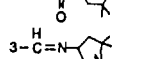
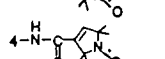
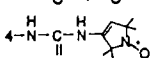
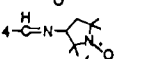
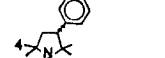
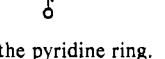
spectrum of the noninteracting nitroxyl obscured the center of the spectrum, the broad signals to low and high field indicated that the exchange interaction was similar for ligands II and XII. The simulated spectrum in Figure 3C was obtained with  $J = 0.0085\text{ cm}^{-1}$ ,  $r = 12\text{ \AA}$ ,  $\epsilon = 5^{\circ}$ , and  $\eta = 75^{\circ}$ . The values of  $r$  obtained for these complexes are similar to what was obtained for the analogous Cu(II)<sup>13</sup> and vanadyl<sup>14</sup> complexes.

In the frozen-solution EPR spectra of Cr(TPP)Cl-X the nitroxyl signal was broadened by interaction with the chromium, but splitting was not resolved. When spin-labeled pyridine I was coordinated to Cr(TPP)Cl, the nitroxyl signal was split into a multiplet with an extent of about 150 G. In these spectra the electron–electron spin–spin interaction is of the order of the nitroxyl nitrogen hyperfine splitting. Adequate simulations would require inclusion of the nitrogen hyperfine splitting. Due to the large amount of computer time that would be required to diagonalize the energy matrix if the nitrogen nuclear spin were included, simulations of these spectra were not attempted. However, it is evident from the spectra that the spin–spin interaction for these complexes is weaker than for the other complexes discussed in this paper.

When ligands V, VII, and IX were coordinated to Cr(TPP)Cl, the nitroxyl signals were severely broadened. Comparison of calculated spectra with the extent of the broad nitroxyl envelope gave only estimates of the magnitude of the exchange interaction, but indicated that  $J$  increased in the order V < VII < II < IX. The lack of resolved features precluded detailed analyses of the spin–spin interaction.

The frozen-solution EPR spectrum of Cr(TPP)Cl-VIII is shown in Figure 4A. The spin–spin interaction splits the nitroxyl signal into components that are shifted to higher and lower field than expected for  $g = 2$ . The spread of these signals is substantially greater than in Figure 3B,C, which indicates that the spin–spin interaction is stronger for ligand VIII than for ligands II or XII. The simulated spectrum in Figure 4A was obtained with  $J = 0.022\text{ cm}^{-1}$ ,  $r = 10\text{ \AA}$ ,  $\epsilon = 35^{\circ}$ , and  $\eta = 5^{\circ}$ . The spread of the nitroxyl signals was significantly greater in the frozen-solution EPR

Table I. Comparison of Exchange Interactions for Cr(TPP)Cl·L and VO(tfac)<sub>2</sub>·L

L	R <sup>a</sup>	Cr(TPP)Cl·L		VO(tfac) <sub>2</sub> ·L	
		nitroxyl line width (RT), G	<i>J</i> (-180 °C), cm <sup>-1</sup>	<i>J</i> (RT), <sup>b</sup> cm <sup>-1</sup>	<i>J</i> (-180 °C), <sup>c</sup> cm <sup>-1</sup>
X		5	small <sup>d</sup>	0.0025	
I		6	small <sup>d</sup>	0.0032	0.00037
V		20	<0.005	0.0088	0.0084
VII		38	~0.005	0.0104	
II		35	0.0073	0.0112	0.0107
XII		40	0.0085	0.0135	
IX		170	~0.01	0.015	
VIII		2 peaks <sup>e</sup>	0.022	0.038	0.037
III		2 peaks <sup>e</sup>	~0.022 <sup>f</sup>	0.040	0.035
VI		2 peaks <sup>e</sup>	~0.022	0.041	
XI		2 peaks <sup>e</sup>	0.037	0.048	
IV		shifted <sup>g</sup>	~0.13	0.17	0.19
XIII		shifted <sup>g</sup>	0.27		

<sup>a</sup>R is the substituent on the pyridine ring. Ligands are listed in order of increasing values of *J* for VO(tfac)<sub>2</sub>·L. <sup>b</sup>Values of *J* at room temperature, taken from ref 12 and 13. If isomers were observed, an average value is given. <sup>c</sup>Values of *J* on imbibed beads at -180 °C, taken from ref 14. <sup>d</sup>Value of *J* comparable in magnitude to the nitrogen nuclear hyperfine splitting. <sup>e</sup>Nitroxyl signal split into two peaks as in Figure 2B. <sup>f</sup>Estimate of *J* based on the similarity among the fluid-solution spectra of the complexes of VIII, VI, and III. The frozen-solution spectrum was poorly defined. <sup>g</sup>Nitroxyl intensity shifted away from *g* = 2, as in Figure 2C.

spectrum of Cr(TPP)Cl·XI (Figure 4B) than in the spectrum in Figure 4A, which indicated an increase in the spin-spin interaction. The simulated spectrum was obtained with *J* = 0.037 cm<sup>-1</sup>, *r* = 10 Å,  $\epsilon$  = 10°, and  $\eta$  = 75°.

Although the simulated spectra in Figure 4A,B indicate that there are turning points at magnetic fields that agree with the experimental spectra, the line widths in the experimental spectra are not matched by the calculated spectra. As the strength of the chromium-nitroxyl interaction increases, the extent of mixing of the chromium and nitroxyl wave functions increases and transitions are not strictly metal or nitroxyl. In the program METNO it is assumed that the line width for a transition is a weighted average of metal and nitroxyl line widths, with the coefficients determined by the relative contributions of metal and nitroxyl operators to the transition probability. It is evident from the discrepancy between the observed and calculated spectra that additional factors need to be considered in assigning the line widths for a transition.

The lines were broader in the frozen-solution EPR spectrum of Cr(TPP)Cl·VI than in the spectrum of Cr(TPP)Cl·VIII, but the spreads of the nitroxyl lines were about the same so the spin-spin interactions were estimated to be similar for the two complexes. The nitroxyl signals in the frozen-solution spectrum of Cr(TPP)Cl·III were not distinguishable from the broad chromium signals. However, since the fluid-solution spectra were similar for the complexes of VIII, III, and VI, it is probable that the spin-spin interactions are similar for the complexes of the three ligands.

The nitroxyl signals were shifted toward the chromium signals to a greater extent in the frozen-solution EPR spectrum of Cr(TPP)Cl·IV than in the spectra in Figure 4A,B. The value of *J* was estimated to be about 0.13 cm<sup>-1</sup>. Since this value of *J* is

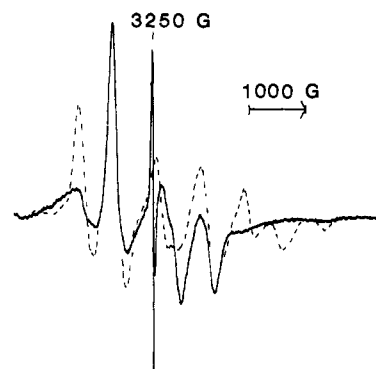


Figure 5. X-Band (9.101 GHz) EPR spectrum (6000-G scan) of Cr(TPP)Cl·XIII in frozen solution at -180 °C, obtained with 4-G modulation amplitude and 20-mW microwave power. The dotted lines indicate regions in which the calculated spectrum does not overlay the experimental curve.

similar in magnitude to *D*, there is extensive crossing of energy levels and the calculated spectra were strongly dependent on the magnetic field at which the diagonalization was done. The value of *J* is therefore quite uncertain for this complex.

The frozen-solution EPR spectrum of Cr(TPP)Cl·XIII is shown in Figure 5. The complexes with the two isomers of XIII gave indistinguishable EPR spectra, which indicated that the orientation of the phenyl substituent had negligible impact on the bonding between the spin-labeled pyridine and the chromium porphyrin. The exchange interaction with this ligand is sufficiently strong that transitions cannot be assigned as metal or nitroxyl. In the limit of strong exchange the  $S = 3/2$ ,  $S = 1/2$  interaction gives

$S = 1$  and  $S = 2$  wave functions. The spectrum in Figure 5 is approaching this limit. The simulated spectrum does not adequately account for the differences in the line widths of the transitions in this limit but does indicate the positions of the turning points in the spectrum. The calculated spectrum was obtained with  $J = 0.27 \text{ cm}^{-1}$ ,  $r = 6 \text{ \AA}$ ,  $\epsilon = 35^\circ$ , and  $\eta = 75^\circ$ . The values of  $r$  and  $\epsilon$  are consistent with CPK molecular models of the complex.

**Trends in the Values of  $J$ .** The values of  $J$  (Table I) were consistently larger for the same substituent at the 4-position of the pyridine ring than at the 3-position, as expected for predominantly  $\pi$  delocalization of the metal unpaired spin density into the pyridine ring. The interaction was weaker through amide linkages than through the Schiff base linkage, which is also consistent with predominantly  $\pi$  delocalization. The stronger interaction for the urea linkage (XI) than for the analogous amide (VI) was observed previously for vanadyl complexes with predominantly  $\pi$  delocalization but not for copper(II) complexes with predominantly  $\sigma$  delocalization.<sup>13</sup> Thus the trends in the values of  $J$  are consistent with  $\pi$  delocalization due to interaction of the partially filled chromium  $d_{xz}$ ,  $d_{yz}$  orbitals with the pyridine  $\pi$  system.

**Comparison with VO(tfac)<sub>2</sub>·L.** Table I summarizes the values of  $J$  that have been obtained for VO(tfac)<sub>2</sub>·L and Cr(TPP)Cl·L. The vanadyl complexes were studied in fluid solution<sup>12,13</sup> and (for some of the ligands) on imbibitor beads at  $-180^\circ\text{C}$ .<sup>14</sup> The values of  $J$  did not appear to be strongly temperature dependent. It therefore seems reasonable to compare these values for the vanadyl complexes with the values of  $J$  obtained for the Cr(TPP)Cl complexes obtained at  $-180^\circ\text{C}$ . The ligands in Table I are arranged in the order of increasing values of  $J$  for the VO(tfac)<sub>2</sub> complexes. The values of  $J$  for the chromium complexes follow the same patterns as the vanadyl complexes. Thus it is evident that the trends in the values of  $J$  observed for one metal with primarily  $\pi$  delocalization into a spin-labeled pyridine are

transferrable to another metal with primarily  $\pi$  delocalization. We had previously observed that trends in the values of  $J$  observed for spin-labeled pyridines bound to two  $S = 1/2$  metals (Cu(II) and low spin Co(II)) with predominantly  $\sigma$  delocalization were similar.<sup>19</sup> Thus it appears that if two metals have similar mechanisms of spin delocalization into the orbitals of the spin-labeled ligand, the trends in the values of  $J$  are similar.

The values of  $J$  for the chromium complexes were about  $1/2$  to  $2/3$  of the values observed for the vanadyl complexes. If the number of unpaired electrons on the metal were the only difference between the two sets of complexes, a factor of  $1/3$  would be expected.<sup>6</sup> The lower oxidation state of the chromium in Cr(TPP)Cl than of vanadium in VO(tfac)<sub>2</sub> may cause a greater spin delocalization of the chromium unpaired electrons than of the vanadyl unpaired electron. Although the geometry of the metalloporphyrin complex is fairly rigidly defined, the geometry of the vanadyl complex may be distorted, thereby decreasing the effectiveness of the overlap between the metal and pyridine orbitals.

**Acknowledgment.** The partial support of this work by NIH Grant GM 21156 is gratefully acknowledged. Purchase of the IBM ER200 EPR spectrometer was funded in part by NSF Grant CHE8411282. Purchase of the Harris H1000 computer was funded in part by a grant from the Harris Corp. We thank Prof. Belford for a copy of his fourth-order frequency shift perturbation routine and for useful discussions concerning its use.

**Registry No.** Cr(TPP)Cl-I, 104090-04-2; Cr(TPP)Cl-II, 104090-05-3; Cr(TPP)Cl-III, 104090-06-4; Cr(TPP)Cl-IV, 104172-20-5; Cr(TPP)Cl-V, 104090-07-5; Cr(TPP)Cl-VI, 104172-21-6; Cr(TPP)Cl-VII, 104113-69-1; Cr(TPP)Cl-VIII, 104090-08-6; Cr(TPP)Cl-IX, 104090-09-7; Cr(TPP)Cl-X, 104090-10-0; Cr(TPP)Cl-XI, 104090-11-1; Cr(TPP)Cl-XII, 104090-12-2; Cr(TPP)Cl-XIII, 104090-13-3.

(19) Eaton, S. S.; Boymel, P. M.; Sawant, B. M.; More, J. K.; Eaton, G. R. *J. Magn. Reson.* 1984, 56, 183.

Contribution from the Department of Chemistry,  
University of Pittsburgh, Pittsburgh, Pennsylvania 15260

## Electron Spin Resonance Studies of Copper(II) Polyamine and Imidazole Complexes

Shirin Siddiqui and Rex E. Shepherd\*

Received August 20, 1985

ESR spectra were obtained in 50:50 Me<sub>2</sub>SO/water glasses for CuL<sub>4</sub><sup>2+</sup> and CuL<sub>5</sub><sup>2+</sup> species (L = imH, imCH<sub>3</sub>, py), for saturated polyamine donors (L = en, trien, tren, cyclam, tet a and tet b), and for mixed-ligand complexes including Cu(en)L<sub>2</sub><sup>2+</sup>, Cu(en)L<sub>3</sub><sup>2+</sup>, Cu(dien)L<sub>2</sub><sup>2+</sup>, Cu(dien)L<sub>3</sub><sup>2+</sup>, Cu(trien)L<sub>2</sub><sup>2+</sup>, Cu(trien)L<sub>3</sub><sup>2+</sup>, and Cu(cyclam)L<sub>2</sub><sup>2+</sup> and Cu(tren)L<sub>2</sub><sup>2+</sup> (L = imH, imCH<sub>3</sub>, or py). The presence of at least one aromatic L donor either in-plane of a CuN<sub>4</sub> donor set (for example Cu(dien)(imH)<sup>2+</sup>) or in the axial position of a CuN<sub>5</sub> donor set (Cu(cyclam)(imH)<sup>2+</sup>) causes all N donors to contribute essentially equally to N-shf patterns in the  $g_{\perp}$  region of the rhombically distorted axial ESR spectrum of the complex. Saturated polyamine complexes exhibit only very weak N-shf coupling in the absence of imidazoles or pyridine. ESR parameters for 36 Cu(II) imidazole, polyamine, or mixed-ligand complexes are reported in the Me<sub>2</sub>SO/water glasses at 113 K. An approximate additivity of the influence of saturated N donors and aromatic N\* donors in various Cu(N,N\*)<sub>4</sub><sup>2+</sup> and Cu(N,N\*)<sub>5</sub><sup>2+</sup> donor sets is observed.

### Introduction

Cu(II) has been termed a "plastic" metal center<sup>1a</sup> due to the ability of a d<sup>9</sup> configuration to take on various modifications of coordination numbers 4, 5, and 6: square planar, tetragonal-

distorted, rhombically distorted tetragonal, trigonal bipyramidal, and distorted octahedral.<sup>2</sup> Although it is convenient to describe complexes such as CuL<sub>4</sub><sup>2+</sup> (L = NH<sub>3</sub>, imH, py, imCH<sub>3</sub>, etc.), Cu(en)<sub>2</sub><sup>2+</sup>, Cu(trien)<sup>2+</sup>, and Cu(dien)L<sub>2</sub><sup>2+</sup> as all CuN<sub>4</sub> species of approximately square-planar geometry, it is known from the sensitivity of ESR spectra that these species are not really equivalent in solution. A question of potential biochemical importance is whether or not one can determine the number of aromatic (imidazole or pyridine type) donor ligands in the presence of saturated N-bases (lysines, amines, etc.) that are present at a Cu(II) site from the ESR spectrum of a copper metalloprotein.

- (1) (a) Gazo, J.; Bersuker, I. B.; Garaj, J.; Kabesova, M.; Kohout, J.; Langfelderova, H.; Melnik, M.; Serator, M.; Valach, F. *Coord. Chem. Rev.* 1976, 19, 253. (b) Margerum, D. W.; Cayley, G. R.; Weatherburn, D. C.; Pagenkopf, G. K. *Coordination Chemistry 2*; ACS Monograph 174; American Chemical Society: Washington, DC, 1978; p 1. (c) Wilkins, R. G. *The Study of Kinetics and Mechanism of Reactions of Transition Metal Complexes*; Allyn and Bacon: Boston, 1974; pp 200-201. (d) Basolo, F.; Pearson, R. G. *Mechanisms of Inorganic Reactions*, 2nd ed.; Wiley: New York, 1967; p 220.

- (2) Hathway, B. J.; Billing, D. E. *Coord. Chem. Rev.* 1970, 5, 143.